THE JOURNAL OF PHYSICAL CHEMISTRY Letters

pubs.acs.org/JPCL

DFT Study of Ligand Binding to Small Gold Clusters

Satyender Goel,[†,‡,∥] Kirill A. Velizhanin,[†,‡] Andrei Piryatinski,[†,‡] Sergei Tretiak,[‡,§] and Sergei A. Ivanov*[,§]

[†]Theoretical Division, and [‡]Center for Nonlinear Studies, [§]Center for Integrated Nanotechnologies, Los Alamos National Laboratory, New Mexico 87545, and [∥]NanoScience Technology Center, University of Central Florida, Orlando, Florida 32826

ABSTRACT The influence of ligands on electronic structure of small gold clusters (Au_2, Au_4) has been investigated by density functional theory (DFT). Specifically, we study the effect of bonding of four donor ligands (NH_3, NMe_3, PH_3, and PMe_3) on cluster geometries and energetics in gas phase and in solution. Performance of five generations of DFT functionals and five different basis sets is assessed. Our results benchmark the importance of the DFT functional model and polarization functions in the basis set for calculations of ligated gold cluster systems. We obtain $NMe_3 \approx NH_3 < PH_3 < PMe_3$ order of ligand binding energies and observe shallow potential energy surfaces in all molecules. The latter is likely to lead to a conformational freedom in larger clusters with many ligands in solution at ambient conditions. The study suggests appropriate quantum-chemical methodology to reliably model small noble metal clusters in a realistic ligand environment typically present in experiments.

SECTION Molecular Structure, Quantum Chemistry, General Theory

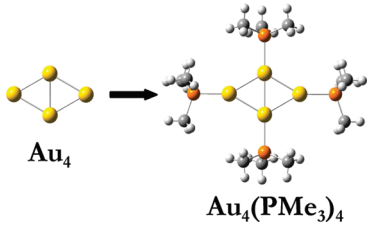

Recently, there has been a significant increase in the research focused on the synthesis, characterization, and theoretical analysis of gold clusters and nanoparticles, as their potential applications encompass ever increasing areas of modern technology and scientific advances, ranging from biological luminophores to the components of plasmonic devices and catalysis. Their ability to guide, enhance, emit, and modify optical fields puts them on the center stage for applications such as photonic crystals, biosensors, and optical materials.[1,2] Small gold clusters (arbitrarily taken here as less than 20 gold atoms) hold promise for great advances in materials science, as they are increasingly viewed as basic elements for assembly of nanoarchitectures having specific emergent properties. On the adopted length scale, the metal clusters become molecular species with discrete electronic states and possible strong fluorescence properties. Several experimental studies done in the past[3,4] explored the high polarizability, optical absorption, and emission properties of these molecular-scale clusters. However, the assignment of the observed spectra is tedious without the detailed knowledge of geometries and associated electronic structures. As the shape and size of nanoclusters define their optical properties, there has been a considerable effort to understand the factors that control the geometry. For example, computational studies of several bare gold nanoclusters (Au_N) suggest transition from two-dimensional (2D) planar structures ($N < 11$) to three-dimensional (3D) systems for $N \geq 13$.[5−7]

Using ligands with functional groups attached to the surface gold atoms allows for the construction of functional nanoassemblies and binding the clusters to surfaces of various substrates. Moreover, the ligand environment could significantly affect the electronic properties of the clusters themselves. Compared to the vast amount of information available for small bare gold clusters, much less theoretical emphasis has been given to the ligation of these clusters with stabilizing molecules—ligands. Previous studies of charged and neutral clusters[8−12] have shown that relative stability can change among 3D isomers as a result of the ligand stabilization effect. For example, Shafai et al.[8] reported the icosahedral (3D) arrangement of gold atoms in Au_{13} as the most stable geometry in the presence of phosphine (PH_3) ligands, whereas the bare cluster is planar. Similar effect was found for Au_{11} cluster in the presence of SCH_3 ligands,[9] which agreed with the experimentally observed 3D structure of a ligand-protected Au_{11} cluster.[13]

This shows that accounting for the ligand effects (or, generally, any surface-adsorbed molecules) is crucial for understanding the behavior of gold clusters observed experimentally. However, it also increases the computational complexity of the problem. A variety of different theoretical chemistry methodologies has been exploited in the past.[5−9,14−21] Even though for bare gold clusters a significant body of theoretical work assesses the performance of different methodologies, no similar studies have been conducted for ligated entities.[1] Acceptable model quantum chemistry should provide reasonable accuracy to infer the leading physical trends and to enable comparison of computational results with experimental data; at the same time, the related

Received Date: January 7, 2010
Accepted Date: February 12, 2010
Published on Web Date: February 24, 2010

DOI: 10.1021/jz1000193 | J. Phys. Chem. Lett. 2010, 1, 927–931

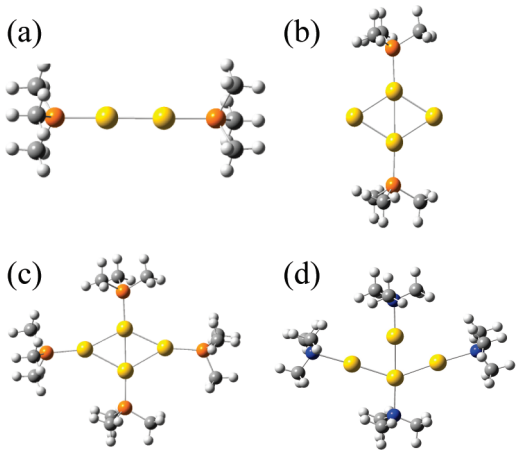

Figure 1. Typical geometries of ligand-protected Au_2 and Au_4 clusters: (a) $Au_2(PMe_3)_2$, (b) $Au_4(PMe_3)_2$, (c) $Au_4(PMe_3)_4$, and (d) $Au_4(NMe_3)_4$. Color scheme: yellow - Au, orange - P, blue - N, dark gray - C, light gray - H.

numerical cost should be low to allow scaling to larger systems. In this work, we explore the effect of different basis sets and density functional theory (DFT) functionals on the geometries and electronic properties of small gold clusters (Au_2 and Au_4) in the presence of several ligands (NH_3, NMe_3, PH_3, and PMe_3). We have tested smaller ligands such as PH_3 for our structural study, as it can satisfactorily model various commonly used alkyl phosphines as well as such ligands as PPh_3, according to previous findings.[22,23] Analysis of the results from different methodologies leads to understanding of the underlying physical phenomena defining cluster geometry and chemical stability, and allows for identification of low-cost computational approaches applicable to larger systems.

Representative geometries of ligated Au_2 and Au_4 clusters are shown in Figure 1. We consider butterfly (rhombus) geometry of the Au_4 cluster, previously found to be the lowest energy isomer.[24] Four types of ligand molecules (NH_3, NMe_3, PH_3, and PMe_3) that can be used in experiment, have been adopted to construct three types of ligated clusters (12 molecules total): Au_2L_2 (e.g., Figure 1a), Au_4L_2 (e.g., Figure 1b), and Au_4L_4 (e.g., Figure 1c,d). We start discussion of the computational results with ligand binding energy, which is a critical quantity showing ligand ability to stabilize a metal cluster. The magnitude of the binding energy has been determined as the difference between the energies of an optimal structure of bound compound and its respective components, that is, free ligand molecules and a bare gold cluster, normalized by the number of ligands in the ligated cluster. Figure 2 shows dependence of the ligand binding energy on the DFT model calculated using the TZVP basis set. Despite the different origin of the five DFT functionals used in our study, the results produced by four of these functionals (with the exception of LSDA) are consistent and in close agreement with each other. Particularly, the binding energies calculated with three functionals (GGA, meta-GGA, and LC-hybrid) are within 2−3 kcal/mol for all clusters (Figure 2). As expected, the LSDA model consistently overestimated the binding energies by about 15 kcal/mol (50−70%) compared to all other models. This is the typical case for many molecular

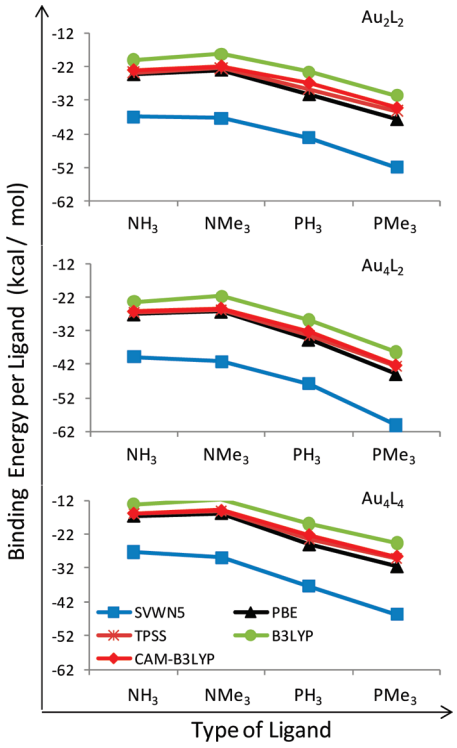

Figure 2. Binding energies per ligand in kcal/mol for geometries of Au_2 and Au_4 in partial and fully ligated forms determined using various DFT functionals. The TZVP basis set was used for all calculations.

systems, when later-developed functional models such as GGA or meta-GGA produce much more accurate results when compared with experimental data.[25] For reference, Table 1S in the Supporting Information provides comparison of the bond lengths and dissociation energies of the bare Au_2 dimer using various functionals with the LANL2DZ basis set: indeed, the LSDA produces the best match to the experimental[26] bond length of Au_2 (2.47 Å), but significantly overestimates the dimer's binding energy. From Figure 2 we also observe that B3LYP slightly underestimates the metal−ligand binding energies by ∼4−5 kcal/mol in all molecules. Overall, we conclude that the ligand binding energy is not overly sensitive to the choice of functional, and the modern DFT models proven reliable for other molecular systems[27,28] are able to provide stable and consistent trends in all considered clusters.

Figure 3 shows the dependence of the ligand binding energy on the basis set size calculated using the TPSS functional. It is apparent that the basis set plays a key role in determining correct energetic trends for ligand binding energies, regardless of the cluster type. Large basis sets (TZVP and QZVP) result in essentially identical ligand binding energies (within 1.5 kcal/mol in all cases). Subsequently, TZVP and QZVP basis sets can be used as reference methods for evaluation of the other three basis sets. We notice that the relative binding strength of amines versus phosphines changes significantly with the change in the basis set flexibility. From all three sets of data in Figure 3, it appears that the lack of polarization in the basis set artificially increases the bonding strength of amine ligands and weakens the bonding

DOI: 10.1021/jz1000193 | J. Phys. Chem. Lett. 2010, 1, 927–931

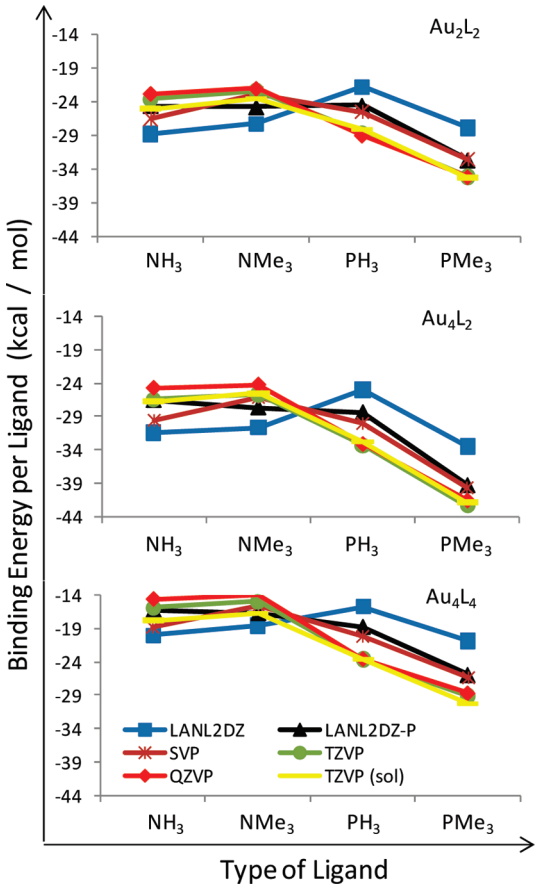

Figure 3. Binding energies per ligand in kcal/mol for geometries of Au_2 and Au_4 in partial and fully ligated forms determined using various basis sets. The TPSS functional was used for all calculations.

of phosphines. The lack of adequate description of polarization effects leads to the underestimation of phosphorus nucleophilicity, thereby lowering the strength of its interaction with gold. At the same time, it leads to artifically high energy of the σ^*(Au−N) antibond, thereby strengthening the bonding of amines with gold. As a result, the least expensive LANL2DZ basis set lacking polarization functions fails to reproduce the relative binding strength of amines versus phosphines. Even adding a single polarization function for each element (LANL2DZ-P) allows one to correct the trend. Notably, both small basis sets, LANL2DZ and LANL2DZ-P, reproduce well the changes in bonding energies for the same family of ligands (NH_3 vs NMe_3) or (PH_3 vs PMe_3). The SVP basis set reproduces well the trend between PH_3 and PMe_3, but not NH_3 vs NMe_3.

The above analysis allows us to select TPSS/TZVP methodology to be adequate to analyze effects of ligand binding to small gold clusters. We further notice, that for all three types of ligated clusters, there is an expected increase in binding energies in the following order of ligands: $NMe_3 \approx NH_3 < PH_3 < PMe_3$. The similar binding energies of NH_3 and NMe_3 are expected because of the high electronegativity of nitrogen that dampens the effect of extra electron density from donating CH_3 groups. The observed similarity is consistent with close values of gas-phase proton affinities of NH_3 and NMe_3 (196 and 216 kcal/mol, respectively).[29] In contrast to amines, the presence of donating groups on phosphorus significantly increases its nucleophilicity, which manifests in higher binding energies of PMe_3 when compared to PH_3. Finally, the radial extend and polarizabilty of the amine lone pair is smaller than that of the phosphine, which in turns leads to weaker binding of amines (23.7 kcal/mol per ligand for Au_2L_2 with TPSS/TZVP) to gold compared to phosphines (28.7 kcal/mol per ligand for Au_2L_2 with TPSS/TZVP). For all ligands we observe an increase in ligand binding energies in the order $Au_4L_4 < Au_2L_2 < Au_4L_2$. The increase in ligand binding from Au_4L_4 to Au_2L_2 most likely comes from increasing nucleophilicty of ligands as their number decreases around the cluster, and the strongest binding of ligands in Au_4L_2 is a result of extra electron density delocalization over four gold atoms compared to only two in Au_2L_2. It is noteworthy that the results produced in the presence of solvent are consistent with above order of binding strengths, but there is an observed increase in binding energies of nitrogen based ligands by 2 kcal/mol for Au_2L_2 and Au_4L_4, whereas there is no such change observed for Au_4L_2. This is likely due to nonuniform changes in cluster structures upon solvation.

The resulting geometries of all ligated clusters are similar and several representative structures are shown in Figure 1. For reference, Table 2S in the Supporting Information presents variations of Au−Au and Au−L bond lengths for the three geometries of the gold clusters we considered determined with different basis sets. The ligation of bare Au_2 dimer with NH_3 and PH_3 leads to an increase of the Au−Au metal bond in the case of PH_3 and does not affect the metal−metal separation in the case of bonding with NH_3. The coordination of two NH_3 or NMe_3 molecules to Au_4 cluster causes shortening of the central Au−Au bond and elongation of four peripheral Au−Au bonds when compared to bare Au_4 geometry. Analysis of bare and ligated Au_2 and Au_4 gold cluster geometries indicates that large basis sets (TZVP and QZVP) can be considered flexible enough to give rise to converged values of both Au−Au and Au−L bond lengths. The LANL2DZ basis set justifiably can be considered the least flexible, as it lacks any polarization functions on either atom. The lack of polarization mostly affects Au−P bonds, whereas Au−N bonds are only slightly elongated. LANL2DZ-P is somewhat less costly than SVP, and its use fixes most shortcomings of the parental LANL2DZ basis, therefore we believe that LANL2DZ-P may be preferred over SVP in geometry optimizations of large ligated gold cluster systems. Relatively small change in nucleophilicity of NMe_3 compared to NH_3 manifests itself only in a weekly pronounced Au−Au bond shrinkage, whereas the strong increase in phosphine nucleophilicity from PH_3 to PMe_3 results in more apparent Au−Au bond elongation.

It is important to note that geometry optimizations usually take many steps to converge since the multidimensional potential energy surfaces are very shallow in all clusters, particularly in the Au_4L_4 case. Consequently, we would expect large conformational freedom in the ligated clusters caused by thermal bath (or solvent) fluctuations. A representative case is the coordination of four ligands to Au_4: we observe that the amine ligand attachment causes an asymmetric shift of the peripheral gold atoms toward one of the central gold

DOI: 10.1021/jz1000193 | J. Phys. Chem. Lett. 2010, 1, 927–931

atoms (Figure 1d) compared to the symmetric structure in the case of phosphine ligands (Figure 1c). This symmetry breaking leads to a significant elongation (~0.15 Å) and weakening of two Au−Au bonds. Even though this conformational change is large, gain in energy due to this symmetry breaking is minimal: the energies of optimal symmetric (when artificial symmetry constraints are imposed) and asymmetric structures are different by 0.4 kcal/mol, which is smaller than the room temperature thermal quantum $kT \sim 0.6$ kcal/mol. Moreover, the introduction of solvent causes Au_4L_4 geometries to appear similar the to Figure 1d structure in the presence of any ligand considered. As such, we expect that large conformational space will be sampled by the ensemble of ligated clusters in solvent.

All calculations have been performed using the commercially available Gaussian09[30] software package. We use five different basis sets with increasing amount of polarization and diffuse functions: the LANL2DZ double-ζ quality basis set with the corresponding effective core potential (ECP),[31] LANL2DZ ECP augmented with single polarization function for each element (LANL2DZ-P),[32,33] the split valence basis set def2-SVP of Ahlrichs et al.[34,35] with polarization, the triple-ζ valence def2-TZVP with polarization, and the quadruple-ζ valence def2-QZVP[36] with polarization on all atoms and corresponding ECP on gold. Several commonly used DFT[37,38] functionals were tested as well. Local spin density approximation (LSDA) was represented by the SVWN5 model, and the generalized gradient approximation (GGA) functional family was represented by the PBE exchange−correlation form. Among the later developed types of DFT functionals, TPSS[39] was our functional of choice for the kinetic energy density-dependent functional (meta-GGA). The currently popular and well-tested B3LYP[40] functional was used as a representative of a hybrid DFT model. B3LYP explicitly contains a fraction (20%) of orbital exchange.[41] Finally, we considered the long-range corrected functional CAM-B3LYP,[27] which accounts for long-range exchange effects believed to be important in the analysis of metal bonding in gold complexes and clusters.[42] Solvation effects were simulated by using implicit CPCM solvation model[43] as implemented in Gaussian 09 with methanol being a solvent of choice. Gas-phase optimized geometries were used as initial guesses to optimize cluster geometries in solution. All geometry optimizations were performed without any symmetry constrains. ChemCraft-(v1.6) and GaussView(v3.0) visualization software packages were used for subsequent visualization of resulting molecular structures.

In conclusion, our computational study of small ligated gold clusters finds weak dependence of geometries and ligand binding energies on DFT functionals used in calculations (except LSDA), while underscoring the importance of polarization functions being present in the utilized basis set. Our results demonstrate that the TPSS/TZVP level of theory (if affordable) would be the method of choice for geometry optimization and chemical energy computations of ligated clusters. The LANL2DZ ECP basis set augmented with one polarization function per element (LANL2DZ-P) can be used for larger systems. We obtain $NMe_3 \approx NH_3 < PH_3 < PMe_3$ order of ligand binding energies for Au_2 and Au_4 clusters. Ligand binding energies also increase in the order $Au_4L_4 < Au_2L_2 < Au_4L_2$ for all ligands. Finally, we observe shallow potential energy surfaces for considered ligated gold cluster Au_4. Consequently, significant conformational freedom in larger clusters with many ligands is expected due to solvent environment fluctuations. This work provides useful computational guidelines and insights for future theoretical and experimental studies toward using ligands as chemical tools to achieve desirable functionalities in noble metal clusters.

SUPPORTING INFORMATION AVAILABLE Table comparing bond lengths and binding energies of Au_2 dimer with different DFT functionals along with Table detailing the Au−Au (peripheral), Au−Au (central), and Au-Ligand bond lengths for 12 clusters of Au_2 and Au_4. This material is available free of charge via the Internet at http://pubs.acs.org.

AUTHOR INFORMATION

Corresponding Author:

*Corresponding author. E-mail: ivanov@lanl.gov.

ACKNOWLEDGMENT This work was supported by the Los Alamos Directed Research and Development (LDRD) funds. We acknowledge support of the Center for Nonlinear Studies (CNLS). This work was performed, in part, at the Center for Integrated Nanotechnologies, a U.S. Department of Energy, Office of Basic Energy Sciences, user facility. Los Alamos National Laboratory is operated by Los Alamos National Security, LLC, for the National Nuclear Security Administration of the U.S. Department of Energy under Contract DE-AC52-06NA25396.

REFERENCES

(1) Pyykkö, P. Theoretical Chemistry of Gold. *Angew. Chem., Int. Ed.* **2004**, *43*, 4412−4456.
(2) Andres, R. P.; Bein, T.; Dorogi, M.; Feng, S.; Henderson, J. I.; Kubiak, C. P.; Mahoney, W.; Osifchin, R. G.; Reifenberger, R. "Coulomb Staircase" at Room Temperature in a Self-Assembled Molecular Nanostructure. *Science* **1996**, *272*, 1323−1325.
(3) Zheng, J.; Zhang, C.; Dickson, R. M. Highly Fluorescent, Water-Soluble, Size-Tunable Gold Quantum Dots. *Phys. Rev. Lett.* **2004**, *93*, 077402−077404.
(4) Zheng, J.; Nicovich, P. R.; Dickson, R. M. Highly Fluorescent Noble-Metal Quantum Dots. *Annu. Rev. Phys. Chem.* **2007**, *58*, 409−431.
(5) Pyykkö, P. Theoretical Chemistry of Gold. III. *Chem. Soc. Rev.* **2008**, *37*, 1967−1997.
(6) Xiao, L.; Tollberg, B.; Hu, X.; Wang, L. Structural Study of Gold Clusters. *J. Chem. Phys.* **2006**, *124*, 114309−114310.
(7) Assadollahzadeh, B.; Schwerdtfeger, P. A Systematic Search for Minimum Structures of Small Gold Clusters Au_n (n = 2−20) and Their Electronic Properties. *J. Chem. Phys.* **2009**, *131*, 064306−064311.
(8) Shafai, G.; Hong, S.; Bertino, M.; Rahman, T. S. Effect of Ligands on the Geometric and Electronic Structure of Au_{13} Clusters. *J. Phys. Chem. C* **2009**, *113*, 12072−12078.
(9) Spivey, K.; Williams, J. I.; Wang, L. Structures of Undecagold Clusters: Ligand Effect. *Chem. Phys. Lett.* **2006**, *432*, 163−166.
(10) Garzón, I. L.; Rovira, C.; Michaelian, K.; Beltrán, M. R.; Ordejón, P.; Junquera, J.; Sánchez-Portal, D.; Artacho, E.;

DOI: 10.1021/jz1000193 | *J. Phys. Chem. Lett.* **2010**, *1*, 927–931

Soler, J. M. Do Thiols Merely Passivate Gold Nanoclusters? *Phys. Rev. Lett.* **2000**, *85*, 5250−5251.
(11) Periyasamy, G.; Remacle, F. Ligand and Solvation Effects on the Electronic Properties of Au_{55} Clusters: A Density Functional Theory Study. *Nano Lett.* **2009**, *9*, 3007−3011.
(12) Wilson, N. T.; Johnston, R. L. Passivated Clusters: A Theoretical Investigation of the Effect of Surface Ligation on Cluster Geometry. *Phys. Chem. Chem. Phys.* **2002**, *4*, 4168−4171.
(13) Yang, Y. Y.; Chen, S. W. Surface Manipulation of the Electronic Energy of Subnanometer-Sized Gold Clusters: An Electrochemical and Spectroscopic Investigation. *Nano Lett.* **2003**, *3*, 75−79.
(14) Bauschlicher, C. W., Jr.; Langhoff, S. R.; Partridge, H. Theoretical Study of the Structures and Electron Affinities of the Dimers and Trimers of the Group IB Metals (Cu, Ag, and Au). *J. Chem. Phys.* **1989**, *91*, 2412−2419.
(15) Bravo-Pérez, G.; Garzón, I. L.; Novaro, O. Ab Initio Study of Small Gold Clusters. *J. Mol. Struct.: THEOCHEM* **1999**, *493*, 225−231.
(16) Wang, J.; Wang, G.; Zhao, J. Density-Functional Study of Au_n (n = 2−20) Clusters: Lowest-Energy Structures and Electronic Properties. *Phys. Rev. B* **2002**, *66*, 035418-6.
(17) Olson, R. M.; Varganov, S.; Gordon, M. S.; Metiu, H.; Chretien, S.; Piecuch, P.; Kowalski, K.; Kucharski, S. A.; Musial, M. Where Does the Planar-to-Nonplanar Turnover Occur in Small Gold Clusters? *J. Am. Chem. Soc.* **2004**, *127*, 1049−1052.
(18) Häkkinen, H.; Landman, U. Gold Clusters (Au_N, $2 < N < 10$) and Their Anions. *Phys. Rev. B* **2000**, *62*, 2287−2290.
(19) Li, X. B.; Wang, H. Y.; Yang, X. D.; Zhu, Z. H.; Tang, Y. J. Size Dependence of the Structures and Energetic and Electronic Properties of Gold Clusters. *J. Chem. Phys.* **2007**, *126*, 084505−084508.
(20) Samah, M.; Bouguerra, M.; Guerbous, L.; Berd, M. DFT Based Study of Au_n (n = 4−7) Clusters: New Stabilized Geometries. *Phys. Scr.* **2007**, *75*, 411−413.
(21) Daniel, M. C.; Astruc, D. Gold Nanoparticles: Assembly, Supramolecular Chemistry, Quantum-Size-Related Properties, and Applications Toward Biology, Catalysis, and Nanotechnology. *Chem. Rev.* **2003**, *104*, 293−346.
(22) Häberlen, O. D.; Rösch, N. Effect of Phosphine Substituents in Gold(I) Complexes: A Theoretical Study of $MeAuPR_3$, R = H, Me, Ph. *J. Phys. Chem.* **1993**, *97*, 4970−4973.
(23) Häberlen, O. D.; Chung, S. C.; Rösch, N. Relativistic Density-Functional Studies of Naked and Ligated Gold Clusters. *Int. J. Quanum Chem. Symp.* **1994**, *52*, 595−610.
(24) Balasubramanian, K.; Feng, P. Y.; Liao, M. Z. Geometries and Energy Separations of 14 Electronic States of Au_4. *J. Chem. Phys.* **1989**, *91*, 3561−3570.
(25) Kanai, Y.; Wang, X.; Selloni, A. Testing the TPSS Meta-Generalized-Gradient-Approximation Exchange-Correlation Functional in Calculations of Transition States and Reaction Barriers. *J. Chem. Phys.* **2006**, *125*, 234104−234108.
(26) Morse, M. D. Clusters of Transition-Metal Atoms. *Chem. Rev.* **2002**, *86*, 1049−1109.
(27) Yanai, T.; Tew, D. P.; Handy, N. C. A New Hybrid Exchange-Correlation Functional Using the Coulomb-Attenuating Method (CAM-B3LYP). *Chem. Phys. Lett.* **2004**, *393*, 51−57.
(28) Staroverov, V. N.; Scuseria, G. E.; Tao, J. M.; Perdew, J. P. Comparative Assessment of a New Nonempirical Density Functional: Molecules and Hydrogen-Bonded Complexes. *J. Chem. Phys.* **2003**, *119*, 12129-9.
(29) Li, J. N.; Fu, Y.; Liu, L.; Guo, Q. X. First-Principle Predictions of Basicity of Organic Amines and Phosphines in Acetonitrile. *Tetrahedron* **2006**, *62*, 11801−11813.
(30) Frisch, M. J.; Trucks, G. W.; Schlegel, H. B.; Scuseria, G. E.; Robb, M. A.; Cheeseman, J. R.; Montgomery, J. A., Jr.; Vreven, T.; Kudin, K. N.; Burant, J. C.; Millam, J. M.; Iyengar, S. S.; Tomasi, J.; Barone, V.; Mennucci, B.; Cossi, M.; Scalmani, G.; Rega, N.; Petersson, G. A.; Nakatsuji, H.; Hada, M.; Ehara, M.; Toyota, K.; Fukuda, R.; Hasegawa, J.; Ishida, M.; Nakajima, T.; Honda, Y.; Kitao, O.; Nakai, H.; Klene, M.; Li, X.; Knox, J. E.; Hratchian, H. P.; Cross, J. B.; Bakken, V.; Adamo, C.; Jaramillo, J.; Gomperts, R.; Stratmann, R. E.; Yazyev, O.; Austin, A. J.; Cammi, R.; Pomelli, C.; Ochterski, J. W.; Ayala, P. Y.; Morokuma, K.; Voth, G. A.; Salvador, P.; Dannenberg, J. J.; Zakrzewski, V. G.; Dapprich, S.; Daniels, A. D.; Strain, M. C.; Farkas, O.; Malick, D. K.; Rabuck, A. D.; Raghavachari, K.; Foresman, J. B.; Ortiz, J. V.; Cui, Q.; Baboul, A. G.; Clifford, S.; Cioslowski, J.; Stefanov, B. B.; Liu, G.; Liashenko, A.; Piskorz, P.; Komaromi, I.; Martin, R. L.; Fox, D. J.; Keith, T.; Al-Laham, M. A.; Peng, C. Y.; Nanayakkara, A.; Challacombe, M.; Gill, P. M. W.; Johnson, B.; Chen, W.; Wong, M. W.; Gonzalez, C.; and Pople, J. A. *Gaussian 03, Revision A.01*; Gaussian Inc.: Wallington CT, 2004.
(31) Hay, P. J.; Wadt, W. R. Ab-Initio Effective Core Potentials for Molecular Calculations - Potentials for K to Au Including the Outermost Core Orbitals. *J. Chem. Phys.* **1985**, *82*, 299−310.
(32) Check, C. E.; Faust, T. O.; Bailey, J. M.; Wright, B. J.; Gilbert, T. M.; Sunderlin, L. S. Addition of Polarization and Diffuse Functions to the LANL2DZ Basis Set for P-Block Elements. *J. Phys. Chem. A* **2001**, *105*, 8111−8116.
(33) Roy, L. E.; Hay, P. J.; Martin, R. L. Revised Basis Sets for the LANL Effective Core Potentials. *J. Chem. Theory Comput.* **2008**, *4*, 1029−1031.
(34) Schafer, A.; Horn, H.; Ahlrichs, R. Fully Optimized Contracted Gaussian Basis Sets for Atoms Like Li to Kr. *J. Chem. Phys.* **1992**, *97*, 2571−2577.
(35) Weigend, F.; Ahlrichs, R. Balanced Basis Sets of Split Valence, Triple Zeta Valence and Quadruple Zeta Valence Quality for H to Rn: Design and Assessment of Accuracy. *Phys. Chem. Chem. Phys.* **2005**, *7*, 3297−3305.
(36) Weigend, F.; Furche, F.; Ahlrichs, R. Gaussian Basis Sets of Quadruple Zeta Valence Quality for Atoms H-Kr. *J. Chem. Phys.* **2003**, *119*, 12753−12762.
(37) Kohn, W.; Becke, A. D.; Parr, R. G. Density Functional Theory of Electronic Structure. *J. Chem. Phys.* **1996**, *100*, 12974−12980.
(38) Kohn, W.; Sham, L. J. Self-Consistent Equations Including Exchange and Correlation Effects. *Phys. Rev.* **1965**, *140*, 1133−1138.
(39) Tao, J. M.; Perdew, J. P.; Staroverov, V. N.; Scuseria, G. E. Climbing the Density Functional Ladder: Nonempirical Meta-Generalized Gradient Approximation Designed for Molecules and Solids. *Phys. Rev. Lett.* **2003**, *91*, 146401−146404.
(40) Becke, A. D. Density-Functional Thermochemistry-3: The Role of Exact Exchange. *J. Chem. Phys.* **1993**, *98*, 5648−5652.
(41) Becke, A. D. Density-Functional Exchange-Energy Approximation with Correct Asymptotic-Behavior. *Phys. Rev. A* **1988**, *38*, 3098−3100.
(42) Akinaga, Y.; Ten-no, S. Range-Separation by the Yukawa Potential in Long-Range Corrected Density Functional Theory with Gaussian-Type Basis Functions. *Chem. Phys. Lett.* **2008**, *462*, 348−351.
(43) Barone, V.; Cossi, M. Quantum Calculation of Molecular Energies and Energy Gradients in Solution by a Conductor Solvent Model. *J. Phys. Chem. A* **1998**, *102*, 1995−2001.

DOI: 10.1021/jz1000193 | *J. Phys. Chem. Lett.* **2010**, *1*, 927–931